

## Inter- and Intramolecular Hydroamination with a Uranium Dialkyl Precursor

Erin M. Broderick, Nathaniel P. Gutzwiller, and Paula L. Diaconescu\*

*Department of Chemistry & Biochemistry, University of California, Los Angeles, California 90095*

*Received July 18, 2009*

The same uranium dibenzyl complex supported by a ferrocene-diamide ligand was used as a precatalyst for both inter- and intramolecular hydroamination reactions. Mechanistic and reactivity studies were undertaken to determine whether the two types of reactions follow the same pathway. The experimental results indicate that more than one mechanism may be operating and that the change in mechanism may be dependent on the type of reaction (inter- versus intramolecular) and/or the type of substrate (primary versus secondary amine). In addition, the synthesis and characterization of a bridging-imide diuranium(IV) complex and of benzyl- and anilide-aryloxide uranium(IV) complexes are reported, and their role in hydroamination reactions is discussed.

### Introduction

Hydroamination, the formal addition of an N–H bond across a carbon–carbon unsaturation, can be achieved in either an inter- or intramolecular fashion to produce nitrogen-containing molecules such as amines, enamines, and imines (Figure 1).<sup>1–8</sup> The importance of the formation of the C–N bond has led to a surge of research in this area.<sup>1</sup> Hydroamination has been shown to occur with early<sup>9–15</sup> or

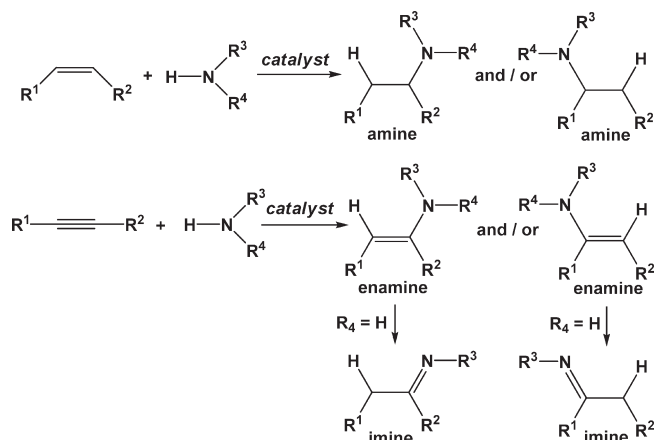


**Figure 1.** Inter-molecular hydroamination reactions producing amines, enamines, and imines.

\*To whom correspondence should be addressed. E-mail: pld@chem.ucla.edu.

- (1) Müller, T. E.; Hultzs, K. C.; Yus, M.; Foubelo, F.; Tada, M. *Chem. Rev.* **2008**, *108*, 3795.
- (2) Müller, T. E.; Beller, M. *Chem. Rev.* **1998**, *98*, 675.
- (3) Alonso, F.; Beletskaya, I. P.; Yus, M. *Chem. Rev.* **2004**, *104*, 3079.
- (4) Hunt, P. A. *Dalton Trans.* **2007**, 1743.
- (5) Aillaud, I.; Collin, J.; Hannedouche, J.; Schulz, E. *Dalton Trans.* **2007**, 5105.
- (6) Seayad, J.; Tillack, A.; Hartung, Christian G.; Beller, M. *Adv. Synth. Catal.* **2002**, *344*, 795.
- (7) Pohlki, F.; Doye, S. *Chem. Soc. Rev.* **2003**, *32*, 104.
- (8) Marks, T. J.; Gagne, M. R.; Nolan, S. P.; Schock, L. E.; Seyam, A. M.; Stern, D. *Pure Appl. Chem.* **1989**, *61*, 1665.
- (9) Lee, A. V.; Schafer, L. L. *Eur. J. Inorg. Chem.* **2007**, 2007, 2245.
- (10) Doye, S. *Synlett* **2004**, 1653.
- (11) Rosenthal, U.; Burlakov, V. V.; Arndt, P.; Baumann, W.; Spannenberg, A.; Shur, V. B. *Eur. J. Inorg. Chem.* **2004**, 2004, 4739.
- (12) Odom, A. L. *Dalton Trans.* **2005**, 225.
- (13) Bytschkov, I.; Doye, S. *Eur. J. Org. Chem.* **2003**, 2003, 935.
- (14) Duncan, A. P.; Bergman, R. G. *Chem. Rec.* **2002**, *2*, 431.
- (15) Siebeneicher, H.; Doye, S. *J. Prakt. Chem.* **2000**, *342*, 102.
- (16) Brunet, J.-J.; Chu, N.-C.; Rodriguez-Zubiri, M. *Eur. J. Inorg. Chem.* **2007**, 2007, 4711.
- (17) Liu, C.; Bender, C. F.; Han, X.; Widenhofer, R. A. *Chem. Commun.* **2007**, 3607.
- (18) Widenhofer, R. A.; Han, X. *Eur. J. Org. Chem.* **2006**, 2006, 4555.
- (19) Mitsudo, T.-A.; Ura, Y.; Kondo, T. *Chem. Rec.* **2006**, *6*, 107.
- (20) Barbaro, P.; Bianchini, C.; Giambastiani, G.; Parisel, S. L. *Coord. Chem. Rev.* **2004**, *248*, 2131.
- (21) Buffat, M. G. P. *Tetrahedron* **2004**, *60*, 1701.
- (22) Hartwig, J. F. *Pure Appl. Chem.* **2004**, *76*, 507.
- (23) Salzer, A. *Coord. Chem. Rev.* **2003**, *242*, 59.
- (24) Hultzs, K. C. *Org. Biomol. Chem.* **2005**, *3*, 1819.
- (25) Gottfriedsen, J.; Edelmann, F. T. *Coord. Chem. Rev.* **2006**, *250*, 2347.

late<sup>16–23</sup> transition metals, as well as with lanthanide<sup>24–31</sup> and actinide<sup>32–40</sup> catalysts.

- (26) Edelmann, F. T. *Coord. Chem. Rev.* **2006**, *250*, 2511.
- (27) Hultzs, K. C.; Gribkov, D. V.; Hampel, F. *J. Organomet. Chem.* **2005**, *690*, 4441.
- (28) Arndt, S.; Okuda, J. *Adv. Synth. Catal.* **2005**, *347*, 339.
- (29) Hong, S.; Marks, T. J. *Acc. Chem. Res.* **2004**, *37*, 673.
- (30) Anwender, R. In *Applied Homogeneous Catalysis with Organometallic Compounds*; Cornils, B., Herrmann, W. A., Eds.; Wiley-VCH: 1996; Vol. 2, p 866.
- (31) Molander, G. A.; Romero, J. A. C. *Chem. Rev.* **2002**, *102*, 2161.
- (32) Eisen, M. S.; Straub, T.; Haskel, A. *J. Alloys Compd.* **1998**, *271–273*, 116.
- (33) Straub, T.; Haskel, A.; Neyroud, T. G.; Kapon, M.; Botoshansky, M.; Eisen, M. S. *Organometallics* **2001**, *20*, 5017.
- (34) Wang, J.; Kumar, A.; Kapon, D. M.; Berthet, J.-C.; Ephritikhine, M.; Eisen, M. S. *Chem.—Eur. J.* **2002**, *8*, 5384.
- (35) Barnea, E.; Eisen, M. S. *Coord. Chem. Rev.* **2006**, *250*, 855.
- (36) Smolensky, E.; Kapon, M.; Eisen, M. S. *Organometallics* **2007**, *26*, 4510.
- (37) Andrea, T.; Eisen, M. S. *Chem. Soc. Rev.* **2008**, *37*, 550.
- (38) Stubbart, B. D.; Stern, C. L.; Marks, T. J. *Organometallics* **2003**, *22*, 4836.
- (39) Stubbart, B. D.; Marks, T. J. *J. Am. Chem. Soc.* **2007**, *129*, 4253.

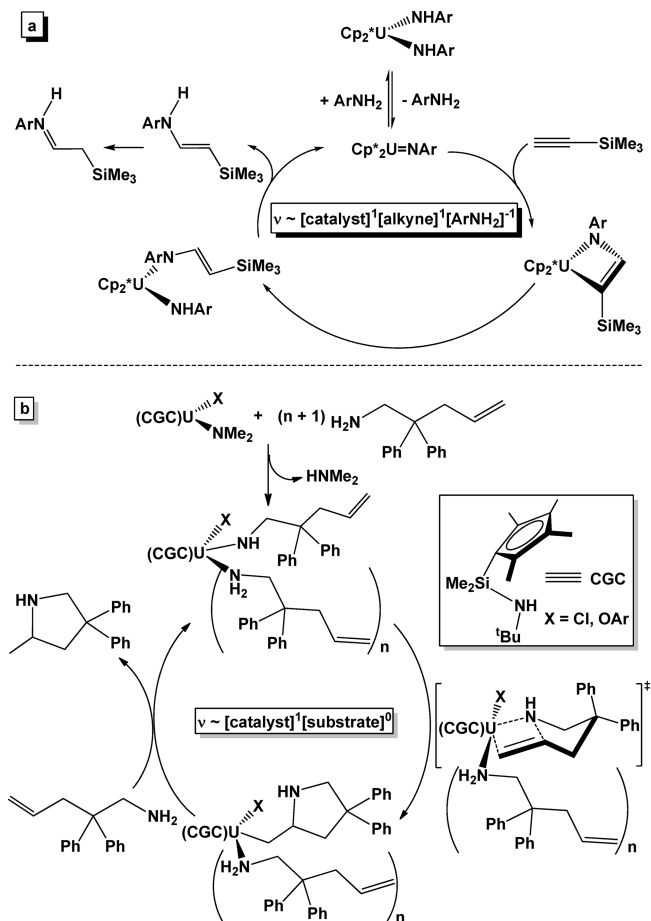


**Figure 2.** (a) Proposed mechanism for the hydroamination of  $\text{Me}_3\text{Si}-\text{C}\equiv\text{CH}$  with aniline in the presence of  $\text{Cp}^*_2\text{U}(\text{NHAr})_2$  (imido mechanism).<sup>33</sup> (b) Proposed mechanism for the reaction of 2,2-diphenyl-4-penten-1-amine in the presence of  $(\text{CGC})\text{U}(\text{NMe}_2)\text{X}$  ( $\text{CGC} = \text{Me}_2\text{Si}(\eta^5-\text{Me}_4\text{C}_5)(^t\text{BuN})$ ,  $\text{X} = \text{Cl}, \text{OAr}$ , amido mechanism).<sup>40</sup>

Two groups, those of Eisen<sup>33</sup> and of Marks,<sup>38–40</sup> have made contributions toward the mechanistic understanding of hydroamination with actinide catalysts. The mechanism proposed by Eisen<sup>33</sup> for the intermolecular hydroamination of alkynes (Figure 2a) involves the formation of a uranium imido intermediate (imido mechanism), similar to group 4 metal examples,<sup>14,41,42</sup> which then undergoes a [2+2] cycloaddition with the olefin to generate an amido-vinyl uranium complex. This complex is protonated by an incoming amine and releases the product; isomerization from the enamine to the imine is generally observed. The mechanism proposed by Marks (Figure 2b) for the intramolecular hydroamination/cyclization of aminoalkenes<sup>39</sup> is similar to that proposed by his group for the analogous reactions using lanthanide catalysts:<sup>29</sup> the intermediate is a uranium amide, which undergoes an olefin migratory-insertion reaction followed by subsequent protonolysis (amido mechanism).

Although both groups show evidence for their proposed mechanisms, the precatalysts used during the kinetics studies are different from one group to the other. Marks et al.

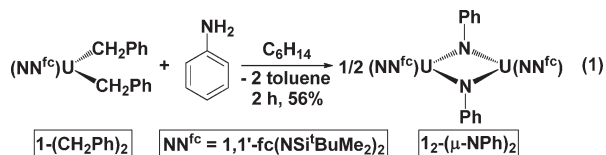
used constrained-geometry (CG) actinide amide complexes,  $(\text{CGC})\text{An}(\text{NMe}_2)\text{X}$  ( $\text{CGC} = \text{Me}_2\text{Si}(\eta^5-\text{Me}_4\text{C}_5)(^t\text{BuN})$ ,  $\text{X} = \text{NMe}_2, \text{OAr}, \text{Cl}$ ),<sup>39,40</sup> while Eisen et al. used a bis(cyclopentadienyl) actinide dialkyl complex,  $\text{Cp}^*_2\text{U}(\text{Me})_2$  ( $\text{Cp}^* = \text{C}_5\text{Me}_5$ ).<sup>33</sup> The complex  $\text{Cp}^*_2\text{U}(\text{Me})_2$  has been used by the Marks group as well, but mechanistic interpretations were extrapolated from experiments using  $(\text{CGC})\text{An}(\text{NMe}_2)\text{X}$ .<sup>39,40</sup>

The goals of the present study are to use the same uranium precatalyst for both inter- and intramolecular hydroaminations and to determine if only one mechanism is operating for a specific type of reaction. Group 4 metal complexes are known to follow either an imido mechanism if they are neutral<sup>41–48</sup> or an amido mechanism if they are cationic,<sup>49–51</sup> with exceptions such as  $(\text{CGC})\text{M}(\text{NMe}_2)\text{X}$  ( $\text{M} = \text{Zr}$ ;  $\text{X} = \text{NMe}_2, \text{Cl}, \text{OAr}$ )<sup>40</sup> and  $\text{Zr}(\text{NMe}_2)_4$ <sup>52</sup> being reported to adopt the amido mechanism. Only a few studies have reported, on the basis of computational and experimental data, both mechanisms to be possible for the same group 4 metal complex.<sup>53,54</sup> For actinide complexes, a computational study with thorium CGC complexes indicated that in the intramolecular hydroamination/cyclization of (4E,6)-heptadienylamine, the amido mechanism is favored over the imido pathway.<sup>55</sup> Herein, we report mechanistic studies of inter- and intramolecular hydroamination reactions using  $\text{fc}(\text{NSi}^t\text{BuMe}_2)_2\text{U}(\text{CH}_2\text{Ph})_2$ , **1**- $(\text{CH}_2\text{Ph})_2$  ( $\text{fc} = 1,1'$ -ferrocenylene),<sup>56</sup> as a precatalyst.

## Results and Discussion

### Synthesis and Characterization of Uranium Complexes.

The synthesis and characterization of the ferrocene-based diamide uranium dialkyl compound **1**- $(\text{CH}_2\text{Ph})_2$  were previously reported by our group.<sup>56</sup> The complex **1**- $(\text{CH}_2\text{Ph})_2$  was synthesized by the reaction of  $\text{KCH}_2\text{Ph}$  with the uranium diiodide complex  $\text{fc}(\text{NSi}^t\text{BuMe}_2)_2\text{U}(\text{I})_2(\text{THF})$ , which, in turn, was obtained from  $\text{UI}_3(\text{THF})_4$ .<sup>57</sup>



Since a uranium terminal imide is proposed to be the catalytically active species in the intermolecular hydroamination

(43) Walsh, P. J.; Hollander, F. J.; Bergman, R. G. *Organometallics* **1993**, *12*, 3705.

(44) Lee, S. Y.; Bergman, R. G. *Tetrahedron* **1995**, *51*, 4255.

(45) Polse, J. L.; Andersen, R. A.; Bergman, R. G. *J. Am. Chem. Soc.* **1998**, *120*, 13405.

(46) Pohlki, F.; Doye, S. *Angew. Chem., Int. Ed.* **2001**, *40*, 2305.

(47) Straub, B. F.; Bergman, R. G. *Angew. Chem., Int. Ed.* **2001**, *40*, 4632.

(48) Tobisch, S. *Chem.—Eur. J.* **2007**, *13*, 4884.

(49) Müller, C.; Koch, R.; Doye, S. *Chem.—Eur. J.* **2008**, *14*, 10430.

(50) Knight, P. D.; Munslow, I.; O'Shaughnessy, P. N.; Scott, P. *Chem. Commun.* **2004**, 894.

(51) Gribkov, D. V.; Hultsch, K. C. *Angew. Chem., Int. Ed.* **2004**, *43*, 5542.

(52) Majumder, S.; Odom, A. L. *Organometallics* **2008**, *27*, 1174.

(53) Müller, C.; Koch, R.; Doye, S. *Chem.—Eur. J.* **2008**, *14*, 10430.

(54) Janssen, T.; Severin, R.; Diekmann, M.; Friedemann, M.; Haase, D.; Saak, W.; Doye, S.; Beckhaus, R. *Organometallics* **2010**, *29*, 1806.

(55) Tobisch, S. *Chem.—Eur. J.* **2010**, *16*, 3441.

(56) Monreal, M. J.; Diaconescu, P. L. *Organometallics* **2008**, *27*, 1702.

(57) Avens, L. R.; Bott, S. G.; Clark, D. L.; Sattelberger, A. P.; Watkin, J. G.; Zwick, B. D. *Inorg. Chem.* **1994**, *33*, 2248.

(40) Stubbert, B. D.; Marks, T. J. *J. Am. Chem. Soc.* **2007**, *129*, 6149.

(41) Walsh, P. J.; Baranger, A. M.; Bergman, R. G. *J. Am. Chem. Soc.* **1992**, *114*, 1708.

(42) Baranger, A. M.; Walsh, P. J.; Bergman, R. G. *J. Am. Chem. Soc.* **1993**, *115*, 2753.

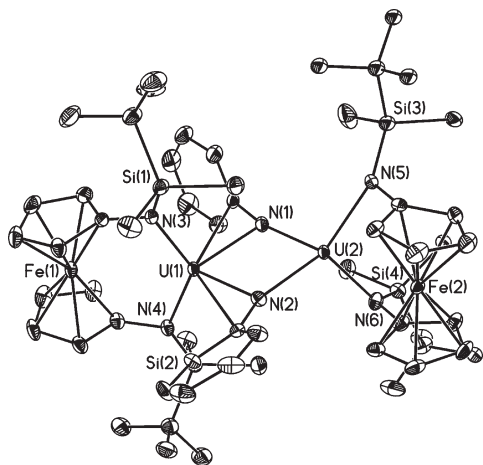


**Figure 3.** Thermal ellipsoid (50% probability) representation of  $1_2-(\mu\text{-NPh})_2$ . Hydrogen atoms were removed for clarity.

reactions,<sup>33</sup> the synthesis and characterization of a uranium-imide complex were attempted. The reaction between  $1-(\text{CH}_2\text{Ph})_2$  and one equivalent of aniline at room temperature led to the isolation of a bridging-imide diuranium(IV) complex,  $1_2-(\mu\text{-NPh})_2$ , in 56% yield after recrystallization from *n*-pentane (eq 1). The complex  $1_2-(\mu\text{-NPh})_2$  shows no signals at room temperature in its  $^1\text{H}$  NMR spectrum,<sup>58</sup> but peaks become visible at 100 °C in toluene- $d_8$ . At this temperature, the chemical shifts are consistent with a symmetrical structure, as inferred from one ancillary ligand environment and one type of imide protons. The X-ray crystal structure of  $1_2-(\mu\text{-NPh})_2$  (Figure 3), however, indicates an unsymmetrical complex, with the phenyl groups of the two bridging imides tilted toward one of the uranium atoms, whereas the other uranium is relatively unobstructed. As a consequence, the latter comes in close contact with the iron center of its ferrocene-diamide ligand (U–Fe, 3.0839(6) Å) and features shorter U–N<sub>imide</sub> distances (2.1666(31) and 2.2449(30) Å) than those to the other uranium atom (2.3320(31) and 2.2563(30) Å). The canting toward one uranium atom is not a consequence of crystal-packing effects (Figure SX1b in the Supporting Information). It is interesting to note that the uranium–iron distance of 3.08 Å in  $1_2-(\mu\text{-NPh})_2$  is as short as the uranium–iron distance (3.08 Å) in  $[\text{fc}(\text{NSi}^t\text{BuMe}_2)_2\text{U}(\text{CH}_2\text{Ph})(\text{OEt}_2)][\text{BPh}_4]$  ( $[\text{1}-(\text{CH}_2\text{Ph})(\text{OEt}_2)][\text{BPh}_4]$ ),<sup>56</sup> indicating a possible interaction<sup>59</sup> between the two metals (the sum of the covalent radii of uranium and iron is 3.28 Å).<sup>60</sup> The uranium–uranium distance of 3.5464(3) Å is also smaller than the sum of the uranium covalent radii (3.92 Å); such short uranium–uranium distances were found for other bridging-imide diuranium(IV) complexes as well.<sup>61–64</sup>

The magnetic properties of  $1_2-(\mu\text{-NPh})_2$  were investigated in order to determine whether the short uranium–uranium distance is accompanied by the coupling of the uranium unpaired electrons. Analyzing the magnetic moment for  $1_2-(\mu\text{-NPh})_2$  in the temperature range 50–300 K (Figure 4), it was noticed that the value corresponding to one uranium was considerably less than that of  $[\text{1}-(\text{CH}_2\text{Ph})(\text{OEt}_2)]-\text{[BPh}_4]$  and of  $1-(\text{CH}_2\text{Ph})_2$  (ca. 1.9 versus 2.4 and 3.2  $\mu_B$ , respectively, at 300 K).<sup>56</sup> In general, for uranium compounds, a smaller value of the room-temperature magnetic moment than the one calculated for the free ion (3.58  $\mu_B$ ) is a consequence of partly quenching the orbital-angular momentum either because of lower symmetry or higher covalency than for the free ion ( $^3\text{H}_4$  for U(IV)).<sup>65</sup> By extrapolation, the magnetic moment value for  $1_2-(\mu\text{-NPh})_2$  indicates a better orbital overlap (higher degree of covalency) in  $1_2-(\mu\text{-NPh})_2$  than in  $1-(\text{CH}_2\text{Ph})_2$  and even in  $1-(\text{CH}_2\text{Ph})(\text{OEt}_2)[\text{BPh}_4]$ , a proposal that is consistent with the short uranium–uranium and iron–uranium distances in  $1_2-(\mu\text{-NPh})_2$ . Since  $1_2-(\mu\text{-NPh})_2$  and  $1-(\text{CH}_2\text{Ph})_2$  feature different coordination environments, however, the low magnetic moment for  $1_2-(\mu\text{-NPh})_2$  may be a consequence of other factors as well. It is noteworthy that the plot of  $\chi T$  versus  $1/T$  (Figure 4) does not show any unusual magnetic behavior for  $1_2-(\mu\text{-NPh})_2$ , ruling out a magnetic exchange between the two uranium centers.

The near-infrared (NIR) spectrum recorded at room temperature for toluene solutions of  $1_2-(\mu\text{-NPh})_2$  showed absorption bands with  $\epsilon \approx 10^2 \text{ M}^{-1} \text{ cm}^{-1}$  (Figure 5). These bands are consistent with f–f transitions,<sup>66,67</sup> a similar spectrum was reported by us for  $1-(\text{CH}_2\text{Ph})_2$  (see the Supporting Information for an overlay of the two spectra).<sup>56</sup> Together with the other characterization data presented here, the NIR spectrum of  $1_2-(\mu\text{-NPh})_2$  indicates that the two uranium centers behave as expected for uranium(IV) complexes with no or little electronic communication between them.

Because the  $^1\text{H}$  NMR spectrum of  $1_2-(\mu\text{-NPh})_2$  at 100 °C was consistent with a symmetrically dinuclear (likely a consequence of enhanced rotation around  $\sigma$  bonds) or a mononuclear complex in solution, but the crystallography studies indicated a dinuclear structure in the solid state, a pulse-gradient spin–echo  $^1\text{H}$  NMR spectroscopy experiment was performed to probe the solution structure.<sup>68</sup> The radius of  $1_2-(\mu\text{-NPh})_2$  was estimated to be 6.8 Å by measuring its diffusion coefficient in a solution of toluene- $d_8$  at 100 °C. This value is close to that calculated from the X-ray crystal structure, 6.9 Å, indicating that  $1_2-(\mu\text{-NPh})_2$  maintains its dinuclear structure in solution at 100 °C.

Next, the observation of a terminal-imide uranium complex from  $1_2-(\mu\text{-NPh})_2$  in the presence of donor molecules was attempted. The reactions of THF, dimethylphenylphosphine, or 2,2'-bipyridine with  $1_2-(\mu\text{-NPh})_2$  were carried out, but  $1_2-(\mu\text{-NPh})_2$  remained unmodified after heating the respective mixtures at 70 °C for several days. Another attempt to isolate a terminal-imide complex was made by

(58) Diaconescu, P. L.; Arnold, P. L.; Baker, T. A.; Mindiola, D. J.; Cummins, C. C. *J. Am. Chem. Soc.* **2000**, *122*, 6108.

(59) Monreal, M. J.; Carver, C. T.; Diaconescu, P. L. *Inorg. Chem.* **2007**, *46*, 7226.

(60) Cordero, B.; Gomez, V.; Platero-Prats, A. E.; Reves, M.; Echeverría, J.; Cremades, E.; Barragan, F.; Alvarez, S. *Dalton Trans.* **2008**, 2832.

(61) Diaconescu, P. L.; Arnold, P. L.; Baker, T. A.; Mindiola, D. J.; Cummins, C. C. *J. Am. Chem. Soc.* **2000**, *122*, 6108.

(62) Stewart, J. L.; Andersen, R. A. *New J. Chem.* **1995**, *19*, 587.

(63) Brennan, J. G.; Andersen, R. A.; Zalkin, A. *J. Am. Chem. Soc.* **1988**, *110*, 4554.

(64) Schnabel, R. C.; Scott, B. L.; Smith, W. H.; Burns, C. J. *J. Organomet. Chem.* **1999**, *591*, 14.

(65) Castro-Rodriguez, I.; Olsen, K.; Gantzel, P.; Meyer, K. *J. Am. Chem. Soc.* **2003**, *125*, 4565.

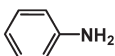
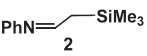
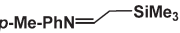
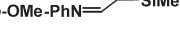
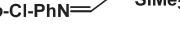
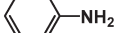
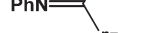
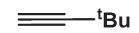
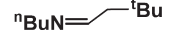
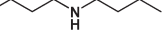
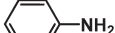
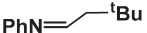
(66) Schelter, E. J.; Yang, P.; Scott, B. L.; Thompson, J. D.; Martin, R. L.; Hay, P. J.; Morris, D. E.; Kiplinger, J. L. *Inorg. Chem.* **2007**, *46*, 7477.

(67) Clark, A. E.; Martin, R. L.; Hay, P. J.; Green, J. C.; Jantunen, K. C.; Kiplinger, J. L. *J. Phys. Chem. A* **2005**, *109*, 5481.

(68) Thérien-Aubin, H.; Baille, W. E.; Zhu, X. X. *Can. J. Chem.* **2008**, *86*, 579.



Table 1. Substrate Scope for Intermolecular Hydroaminations with  $1-(\text{CH}_2\text{Ph})_2$ <sup>a</sup>

entry	alkyne/olefin	amine	product	time	conversion
1				32 min	90%
2				50 min	87%
3				20 h <sup>b,c</sup>	96%
4				20 h <sup>b,c</sup>	95%
5			N.R. <sup>c</sup>		
6				3 h	70%
7				3 d	48%
8				3 d	18%
9			N.R. <sup>c</sup>		
10				3 d	7%

<sup>a</sup> Reactions were performed in  $\text{C}_6\text{D}_6$  at 70 °C with 10 mol %  $1-(\text{CH}_2\text{Ph})_2$ ; [catalyst] = 4.0 mM, [alkyne] = 0.40 M, [amine] = 0.04 M. <sup>b</sup> Room temperature. <sup>c</sup> [catalyst] = 1.7 mM, [alkyne] = 0.34 M, [amine] = 0.034 M.

presence of catalytic amounts of  $1-(\text{CH}_2\text{Ph})_2$  to give the expected hydroamination products (Table 1). Several reactions between  $\text{Me}_3\text{Si}-\text{C}\equiv\text{CH}$  and aniline derivatives were successful (entries 1–4), as well as the reaction with *n*-butylamine (entry 6). A large-scale hydroamination reaction of aniline and  $\text{Me}_3\text{Si}-\text{C}\equiv\text{CH}$  with  $1-(\text{CH}_2\text{Ph})_2$  led to the isolation of the product **2** in 74% yield, indicating that only one of the two possible regioisomers is formed in this reaction. When the alkyne was changed to  $^n\text{Bu}-\text{C}\equiv\text{CH}$ , the reaction with aniline required three days to obtain a 48% conversion to the imine product (entry 7). Similarly, when the alkyne was replaced by  $^t\text{Bu}-\text{C}\equiv\text{CH}$ , only a low conversion with either *n*-butylamine (entry 8) or aniline (entry 10) was observed after three days. No hydroamination products were observed in the reactions of aniline with styrene, norbornene, phenylacetylene, 2-phenylpropyne, 2-butyne, or diphenylacetylene or in the reaction of *n*-butylamine with diphenylacetylene, but such results are not surprising given that these are difficult substrates in intermolecular hydroaminations. The formation of alkyne oligomers was observed in the reactions that did not lead to hydroamination products, similarly to the results reported by Eisen et al.<sup>33</sup> The alkyne-oligomerization products were also obtained independently from the reactions of  $1-(\text{CH}_2\text{Ph})_2$  with alkynes, such as  $\text{Me}_3\text{Si}-\text{C}\equiv\text{CH}$  and 1-hexyne (see the Supporting Information for details).

It is worth mentioning that the Eisen group reported all the intermolecular hydroaminations catalyzed by uranium complexes to occur between unhindered aliphatic (as opposed to aromatic) amines and terminal acetylenes.<sup>33</sup> Only one example of a reaction between  $^i\text{Pr}-\text{C}\equiv\text{CH}$  and aniline was reported that was catalyzed by  $\text{Cp}^*\text{ThMe}_2$ ; that reaction mixture converted 95% to the corresponding imine after 170 h of heating at 78 °C. A similar situation was encoun-

tered for intermolecular hydroaminations with group 4 metal complexes involving anilines and alkynes, which, in general, required temperatures above 100 °C and prolonged heating.<sup>69–80</sup> The scope of the intermolecular hydroaminations performed by us was limited by the fact that  $1-(\text{CH}_2\text{Ph})_2$  was not stable above 70 °C for long periods of time<sup>56</sup> and decomposed when the reaction mixtures were heated above that temperature.

Next, it was observed that there was no reaction between  $\text{Me}_3\text{Si}-\text{C}\equiv\text{CH}$  and *N*-methylaniline (entry 5) or dibutylamine (entry 9), suggesting that in those reactions a terminal uranium(IV) imide<sup>81–86</sup> may be the catalytically active

(69) Heutling, A.; Pohlki, F.; Doye, S. *Chem.—Eur. J.* **2004**, *10*, 3059.

(70) Shi, Y.; Ciszewski, J. T.; Odom, A. L. *Organometallics* **2001**, *20*, 3967.

(71) Shi, Y.; Ciszewski, J. T.; Odom, A. L. *Organometallics* **2002**, *21*, 5148.

(72) Cao, C.; Ciszewski, J. T.; Odom, A. L. *Organometallics* **2001**, *20*, 5011.

(73) Shi, Y.; Hall, C.; Ciszewski, J. T.; Cao, C.; Odom, A. L. *Chem. Commun.* **2003**, 586.

(74) Ackermann, L. *Organometallics* **2003**, *22*, 4367.

(75) Ong, T.-G.; Yap, G. P. A.; Richeson, D. S. *Organometallics* **2002**, *21*, 2839.

(76) Tillack, A.; Jiao, H.; Castro, I. G.; Hartung, C. G.; Beller, M. *Chem.—Eur. J.* **2004**, *10*, 2409.

(77) Wang, H.; Chan, H.-S.; Xie, Z. *Organometallics* **2005**, *24*, 3772.

(78) Li, C.; Thomson, R. K.; Gillon, B.; Patrick, B. O.; Schafer, L. L. *Chem. Commun.* **2003**, 2462.

(79) Bexrud, J. A.; Li, C.; Schafer, L. L. *Organometallics* **2007**, *26*, 6366.

(80) Lorber, C.; Choukroun, R.; Vendier, L. *Organometallics* **2004**, *23*, 1845.

(81) Arney, D. S. J.; Burns, C. J. *J. Am. Chem. Soc.* **1995**, *117*, 9448.

(82) Arney, D. S. J.; Burns, C. J.; Smith, D. C. *J. Am. Chem. Soc.* **1992**, *114*, 10068.

(83) Arney, D. S. J.; Burns, C. J. *J. Am. Chem. Soc.* **1993**, *115*, 9840.

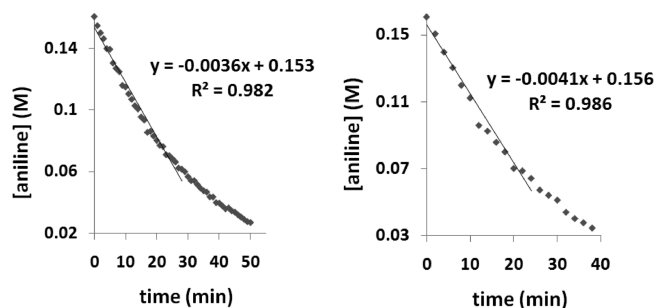


**Figure 7.** Determination of the reaction order in amine concentration for the hydroamination of  $\text{Me}_3\text{Si}-\text{C}\equiv\text{CH}$  and aniline catalyzed by  $\mathbf{1-(CH_2Ph)_2}$  (left) and  $\mathbf{1_2-(\mu-NPh)_2}$  (right) at  $70^\circ\text{C}$  in  $\text{C}_6\text{D}_6$ .

species (an intermolecular hydroamination reaction between  $\text{Me}_3\text{Si}-\text{C}\equiv\text{CH}$  and  $\text{Et}_2\text{NH}$ , catalyzed by  $[(\text{Et}_2\text{N})_3(\text{Et}_2\text{NH})_3\text{U}]^+$ , was reported, but a detailed mechanistic study was not carried out).<sup>34</sup> In order to probe whether this hypothesis extends to the reaction of  $\mathbf{1-(CH_2Ph)_2}$  with  $\text{Me}_3\text{Si}-\text{C}\equiv\text{CH}$  and aniline, the reaction between those substrates was carried out using  $\mathbf{1_2-(\mu-NPh)_2}$  as a precatalyst (1.2 mol %). Even though a terminal-imide uranium(IV) complex could not be obtained from  $\mathbf{1_2-(\mu-NPh)_2}$ , the product **2** (78% conversion) was obtained after 38 min at  $70^\circ\text{C}$ , similar to what was found when  $\mathbf{1-(CH_2Ph)_2}$  was used as a precatalyst. Furthermore, the observed reaction rate of  $6.8 \times 10^{-5} \text{ M s}^{-1}$  (Figure 7) was the same as that determined for  $\mathbf{1-(CH_2Ph)_2}$  ( $6.0 \times 10^{-5} \text{ M s}^{-1}$ , see below). The reactions of 2-butyne with aniline or di-*n*-butylamine with  $\text{Me}_3\text{Si}-\text{C}\equiv\text{CH}$  in the presence of  $\mathbf{1_2-(\mu-NPh)_2}$  gave the same results as those conducted in the presence of  $\mathbf{1-(CH_2Ph)_2}$  (no reaction), indicating that  $\mathbf{1-(CH_2Ph)_2}$  and  $\mathbf{1_2-(\mu-NPh)_2}$  are proceeding through a similar mechanism in these reactions and that a terminal-imide uranium complex is likely the catalytically active species. It is also noteworthy that the reaction of  $\text{Me}_3\text{Si}-\text{C}\equiv\text{CH}$  and aniline mediated by  $\mathbf{1-(CH_2Ph)_2}$  occurred faster when lower concentrations of aniline were used than when higher concentrations of aniline were employed, consistent with the formation of a terminal imide as the active catalyst, although these results are also consistent with the interpretation that aniline may inhibit a  $\sigma$ -bond migratory-insertion step (that is part of the amido mechanism).

The reaction between aniline and  $\text{Me}_3\text{Si}-\text{C}\equiv\text{CH}$  in the presence of  $\mathbf{1-(CH_2Ph)(OAr)}$  was also attempted because it was reasoned that this precatalyst would not be able to form a uranium imide. As described earlier,  $\mathbf{1-(CH_2Ph)(OAr)}$  reacts with one equivalent of aniline to give the anilide-aryloxide complex  $\mathbf{1-(NHPh)(OAr)}$  (eq 3). Even when three equivalents of aniline were used,  $\mathbf{1-(NHPh)(OAr)}$  was the only product after the reaction mixture was heated for several days at  $70^\circ\text{C}$ . The latter experiment was performed because it was observed that aniline can protonate aryloxides smaller than 2,6-di-*tert*-butylphenol (see above). These experiments indicate that the anilide-aryloxide complex can be formed from  $\mathbf{1-(CH_2Ph)_2}$ , but the bis(amide) complex cannot. Consequently, when  $\text{Me}_3\text{Si}-\text{C}\equiv\text{CH}$  (1800 equivalents) and aniline

(80 equivalents) were added to  $\mathbf{1-(CH_2Ph)(OAr)}$ , no conversion to **2** was observed after one day at  $70^\circ\text{C}$  in  $\text{C}_6\text{D}_6$ . This finding is consistent with two mechanistic scenarios: (1) the precatalyst  $\mathbf{1-(CH_2Ph)_2}$  accesses the imido mechanism for intermolecular-hydroamination reactions and (2) either type of reaction (imido or amido mechanism) is suppressed with  $\mathbf{1-(CH_2Ph)(OAr)}$  because the steric bulk of the aryloxide ligand prevents the coordination of the two substrates.

Furthermore, it was investigated whether a migratory insertion of the alkyne into the U–N bond of  $\mathbf{1_2-(\mu-NPh)_2}$  may occur. The addition of excess  $\text{Me}_3\text{Si}-\text{C}\equiv\text{CH}$  to  $\mathbf{1_2-(\mu-NPh)_2}$  and heating of the reaction mixture at  $70^\circ\text{C}$  for one day resulted in no change to the bridging-imide uranium complex, indicating that the intermolecular hydroamination reactions do not initiate with the alkyne substrate.

Kinetics studies were conducted with  $\text{Me}_3\text{Si}-\text{C}\equiv\text{CH}$ , aniline, and  $\mathbf{1-(CH_2Ph)_2}$  at  $70^\circ\text{C}$  in  $\text{C}_6\text{D}_6$  and monitored by  $^1\text{H}$  NMR spectroscopy. In order to determine the order in amine, the catalyst concentration was held constant, while the alkyne to amine ratio was held at a value greater than 12:1 to minimize amine inhibition and maintain pseudo-first-order conditions. Although the reaction was followed until 90% conversion of aniline, the kinetics data were only considered until 60% conversion because the plot of [aniline] versus time curved around that value. It is possible that two different mechanisms operate during the two time ranges, although most reports indicate that product inhibition occurs toward the end of hydroamination reactions. In order to probe whether product inhibition takes place in the above reactions, two experiments were carried out:

(1) The reaction of  $\mathbf{1-(CH_2Ph)_2}$  with 1400 equivalents of  $\text{Me}_3\text{Si}-\text{C}\equiv\text{CH}$  and 80 equivalents of aniline was performed, and then another 80 equivalents of aniline was added. The first reaction occurred fast until ca. 60% conversion of aniline, and then it slowed down. The addition of fresh aniline caused the reaction rate to increase, but the product formation was about 10% slower than in the initial reaction.

(2) The reaction between  $\mathbf{1-(CH_2Ph)_2}$  and 1400 equivalents of  $\text{Me}_3\text{Si}-\text{C}\equiv\text{CH}$  and 80 equivalents of aniline was carried out in the presence of 80 equivalents of the product **2**. It was observed that the reaction proceeded slower in its presence than in its absence (after 20 min, the reaction without **2** present showed 30% conversion, while the reaction with **2** present had 20% conversion), indicating that the product may be inhibiting the reaction.

The disappearance of the aryl-proton resonances for the aniline was normalized to an internal standard, hexaethylbenzene. The kinetics data plot in Figure 7 shows a linear dependence of [aniline] versus time, indicating a zero-order dependence on amine concentration. Given that  $\mathbf{1-(CH_2Ph)_2}$  forms  $\mathbf{1_2-(\mu-NPh)_2}$  within minutes at room temperature, the zero-order dependence on amine concentration is not surprising. Although an inverse order in amine concentration was reported by the Eisen group in analogous reactions, a kinetics analysis of the imido mechanism indicates that the rate law obtained here is in agreement with a fast pre-equilibrium or irreversible formation of the imide intermediate, followed by a fast [2+2] cycloaddition reaction with the alkyne.<sup>40,42</sup>

In order to determine the order in catalyst, the initial concentrations of the alkyne and amine were held constant, while the concentration of  $\mathbf{1-(CH_2Ph)_2}$  was varied over a 6-fold range. Outside of this range, reactions were inconsistent, possibly due to catalyst decomposition as a consequence of

(84) Haskel, A.; Straub, T.; Eisen, M. S. *Organometallics* **1996**, *15*, 3773.

(85) Zi, G.; Blosch, L. L.; Jia, L.; Andersen, R. A. *Organometallics* **2005**, *24*, 4602.

(86) Barros, N.; Maynau, D.; Maron, L.; Eisenstein, O.; Zi, G.; Andersen, R. A. *Organometallics* **2007**, *26*, 5059.

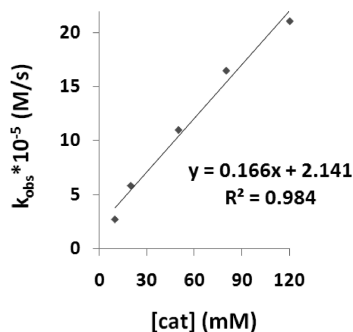


**Figure 8.** Determination of the reaction order in catalyst concentration for the intermolecular hydroamination of  $\text{Me}_3\text{Si}-\text{C}\equiv\text{CH}$  and aniline in the presence of  $1-(\text{CH}_2\text{Ph})_2$  in  $\text{C}_6\text{D}_6$  at  $70^\circ\text{C}$ .

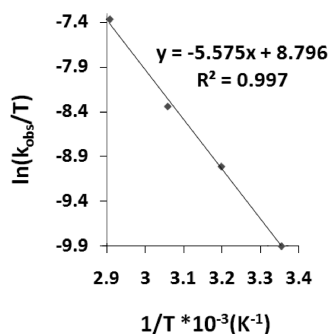


**Figure 9.** Eyring plot for the hydroamination of  $\text{Me}_3\text{Si}-\text{C}\equiv\text{CH}$  with aniline in the presence of 7.5 mol % of  $1-(\text{CH}_2\text{Ph})_2$  in  $\text{C}_6\text{D}_6$ .

the large amount of aniline present. A plot of the reaction rate,  $k_{\text{obs}}$ , versus precatalyst concentration indicates a first-order dependence on  $[1-(\text{CH}_2\text{Ph})_2]$  (Figure 8). Finally, when the concentrations of the amine and precatalyst were held constant and the concentration of the alkyne was changed over a 6-fold range, the rate of the reaction stayed the same. Therefore, the rate law for the intermolecular hydroamination of  $\text{Me}_3\text{Si}-\text{C}\equiv\text{CH}$  with aniline in the presence of  $1-(\text{CH}_2\text{Ph})_2$  is  $\nu = k[1-(\text{CH}_2\text{Ph})_2]^1[\text{alkyne}]^0[\text{amine}]^0$ . Consistent with the fact that the amine is not present in the rate law and that the N–H bond does not participate in the rate-determining step, the observed reaction rate when  $\text{C}_6\text{H}_5\text{ND}_2$  was used in a reaction with  $\text{Me}_3\text{Si}-\text{C}\equiv\text{CH}$  and  $1-(\text{CH}_2\text{Ph})_2$  was similar to the rate for the aniline reaction ( $k_{\text{H}}/k_{\text{D}} = 1.03$ ).

A temperature-dependent study (Figure 9) allowed the determination of the activation parameters  $\Delta H^\ddagger = 11.0(1)$  kcal/mol,  $\Delta S^\ddagger = -30(3)$  eu, and  $E_a = 11.7(1)$  kcal/mol for the reaction of  $\text{Me}_3\text{Si}-\text{C}\equiv\text{CH}$  with aniline in the presence of  $1-(\text{CH}_2\text{Ph})_2$ . These values are similar to those reported by the Eisen group for the hydroamination of  $\text{Me}_3\text{Si}-\text{C}\equiv\text{CH}$  and  $\text{EtNH}_2$  mediated by  $\text{Cp}^*_2\text{UMe}_2$  ( $\Delta H^\ddagger = 11.7(3)$  kcal/mol and  $\Delta S^\ddagger = -44.5(8)$  eu).<sup>33</sup> Therefore, on the basis of all the data presented above, the difference in the order of the amine concentration notwithstanding, the mechanism proposed by us is analogous to that proposed by Eisen et al. for the intermolecular hydroamination of alkynes.<sup>33</sup> Since  $1_2-(\mu\text{-NPh})_2$  was very reluctant to form monomeric adducts, it is proposed that the rate-determining step in the reaction of  $\text{Me}_3\text{Si}-\text{C}\equiv\text{CH}$  with aniline in the presence of  $1-(\text{CH}_2\text{Ph})_2$  is the formation of the terminal imide from the dinuclear complex  $1_2-(\mu\text{-NPh})_2$ , consistent with a zero-order dependence on both the amine and alkyne substrate and a first-order dependence on precatalyst concentration.

**Table 2. Substrate Scope for the Intramolecular Hydroamination/Cyclization Reaction with  $1-(\text{CH}_2\text{Ph})_2$ <sup>a</sup>**

substrate	product	time	conversion
		22 min <sup>b</sup>	88%
		3 d <sup>b</sup>	80%
		10 min <sup>c</sup>	99%

<sup>a</sup> Reactions were performed in  $\text{C}_6\text{D}_6$  at  $70^\circ\text{C}$ . <sup>b</sup> [catalyst] = 11.2 mM, [3a/b] = 0.45 M. <sup>c</sup> [catalyst] = 6.0 mM, [3c] = 0.45 M, room temperature.

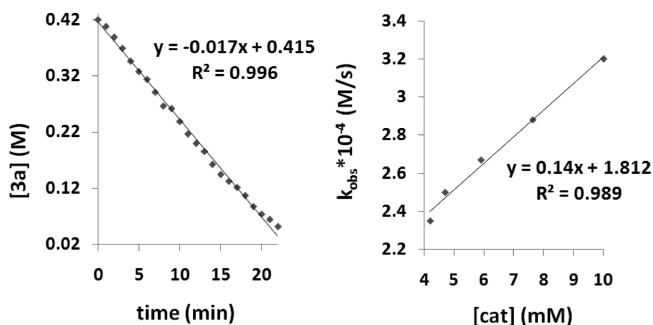


**Figure 10.** Determination of the reaction order in amine (left) and catalyst (right) for the reaction of 2,2-diphenyl-4-penten-1-amine (**3a**) with  $1-(\text{CH}_2\text{Ph})_2$  in  $\text{C}_6\text{D}_6$  at  $70^\circ\text{C}$ .

#### Intramolecular Hydroamination/Cyclization Reactions.

The complex  $1-(\text{CH}_2\text{Ph})_2$  was also used as a precatalyst for the intramolecular hydroamination/cyclization of 2,2-diphenyl-4-penten-1-amine (**3a**) to give the corresponding cyclic product **4a** in 22 min at  $70^\circ\text{C}$  in  $\text{C}_6\text{D}_6$  (Table 2). A large-scale reaction of **3a** with  $1-(\text{CH}_2\text{Ph})_2$  (18 mol %) resulted in the isolation of **4a** in a 70% yield.

Unlike what was found for the intermolecular hydroamination (see above), when the secondary amine *N*-methyl-2,2-diphenyl-4-penten-1-amine (**3b**) was used, the formation of the cyclized product **4b** was observed, although the reaction had to be heated at  $70^\circ\text{C}$  in  $\text{C}_6\text{D}_6$  for three days to achieve an 80% conversion. Similar observations have been reported for analogous reactions catalyzed by actinide complexes.<sup>40</sup> In order to compare directly the reactions of alkyne substrates, the reaction between 2,2-diphenyl-4-pentyn-1-amine (**3c**) and  $1-(\text{CH}_2\text{Ph})_2$  (Table 2) was also carried out, leading to the formation of the expected product, **3d**, at room temperature within minutes.

Kinetics studies were conducted for the reaction between **3a** and  $1-(\text{CH}_2\text{Ph})_2$ . The disappearance of the peak for the terminal olefinic protons, at 5.2 ppm, was monitored by  $^1\text{H}$  NMR spectroscopy (the peaks were normalized to the internal standard hexaethylbenzene). The plot of **[3a]** versus time indicated a zero-order dependence for the substrate concentration (Figure 10). To determine the order in catalyst, **[3a]** was kept constant and the concentration of  $1-(\text{CH}_2\text{Ph})_2$  was varied over a 2.5-fold range. A linear plot of the rate versus **[1-(CH<sub>2</sub>Ph)<sub>2</sub>]** indicated a first-order dependence on the precatalyst concentration (Figure 10). Therefore, the rate law for the intramolecular hydroamination/cyclization of **3a** in the presence of  $1-(\text{CH}_2\text{Ph})_2$  is  $\nu = k[\text{3a}]^0[1-(\text{CH}_2\text{Ph})_2]^1$ .

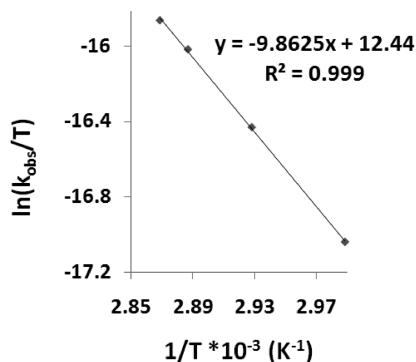


**Figure 11.** Eyring plot for the hydroamination of 2,2-diphenyl-4-penten-1-amine (**3a**) with **1-(CH<sub>2</sub>Ph)<sub>2</sub>** (1.4 mol %) in C<sub>6</sub>D<sub>6</sub>.

Consistent with this rate law, when 2,2-diphenyl-4-penten-1-amine-*d*<sub>2</sub> was used, only a small difference in the rate of its reaction with **1-(CH<sub>2</sub>Ph)<sub>2</sub>** was observed by comparison to the rate for the reaction between **3a** and **1-(CH<sub>2</sub>Ph)<sub>2</sub>** ( $k_H/k_D = 1.36$ ). These data are consistent with either one of the two situations:

(1) The turnover-limiting step is the intramolecular amide migratory insertion into the C=C bond, analogous to the reaction pathway proposed previously for aminoalkene hydroamination/cyclization by uranium complexes (amido mechanism).<sup>39,40</sup> The fact that **3b** reacted with **1-(CH<sub>2</sub>Ph)<sub>2</sub>** supports this mechanism.

(2) The turnover-limiting step is the metallacycle formation ([2+2] cycloaddition with a uranium imide), analogous to the reaction pathway proposed above for the intermolecular hydroamination. The fact that **3b** required a significantly longer time than **3a** to react with **1-(CH<sub>2</sub>Ph)<sub>2</sub>** indicates that the mechanisms of the two reactions may be different.

An Eyring plot shows  $\Delta H^\ddagger = 19.5(1)$  kcal/mol,  $\Delta S^\ddagger = -22(2)$  eu, and  $E_a = 20.3(1)$  kcal/mol for the reaction of **3a** with **1-(CH<sub>2</sub>Ph)<sub>2</sub>** (Figure 11). These values are similar to those reported for the reaction of the dimethyl analogue of **3a** with (CGC)An(N[SiMe<sub>3</sub>]<sub>2</sub>)Cl ( $\Delta H^\ddagger = 16(3)$  kcal/mol,  $\Delta S^\ddagger = -18(9)$  eu, and  $E_a = 17(3)$  kcal/mol) and in the range of those observed for intramolecular hydroamination reactions catalyzed by lanthanide catalysts.<sup>40</sup> It is important to note, however, that the activation parameters are relatively similar for the two types of reactions (intra- and intermolecular).

The complexes **1-(CH<sub>2</sub>Ph)(OAr)** and **1<sub>2</sub>-(μ-NPh)<sub>2</sub>** were also employed in intramolecular hydroamination/cyclization reactions. The reactions of **3a** and **3c** in the presence of **1-(CH<sub>2</sub>Ph)(OAr)** led to the formation of the products **4a** and **4c** after two days and one hour, respectively. The complex **1-(CH<sub>2</sub>Ph)(OAr)** (10 mol %) also reacted with **3b**, and 10% conversion was achieved after four days at 70 °C in C<sub>6</sub>D<sub>6</sub>. All reactions required longer times than when **1-(CH<sub>2</sub>Ph)<sub>2</sub>** was used to achieve similar conversions, indicating that either the results are a consequence of the sterically hindered aryloxide ligand or that a change in mechanism occurs from **1-(CH<sub>2</sub>Ph)(OAr)** to **1-(CH<sub>2</sub>Ph)<sub>2</sub>**.

When **1<sub>2</sub>-(μ-NPh)<sub>2</sub>** (1.8 mol %) was used as a precatalyst in reactions with **3a** and **3c**, the results were surprising: the substrate **3a** was 70% converted in 7.5 h at 70 °C in C<sub>6</sub>D<sub>6</sub>, while a 99% conversion of **3c** was achieved within 10 minutes at room temperature. The complex **1<sub>2</sub>-(μ-NPh)<sub>2</sub>** also converted **3b** (11% in four days). The conversion of **3b** indicates

that **1<sub>2</sub>-(μ-NPh)<sub>2</sub>** may form an amide or bis(amide) species under these reaction conditions that acts as a catalyst, a hypothesis supported by the fact that the reaction of **3a** with **1<sub>2</sub>-(μ-NPh)<sub>2</sub>** showed a large induction period (3% conversion after one hour). The induction period is consistent with the fact that, in the reaction of **1-(CH<sub>2</sub>Ph)<sub>2</sub>** with aniline, **1<sub>2</sub>-(μ-NPh)<sub>2</sub>** forms immediately and a bis(amide) complex could not be isolated (see above). Therefore, on the basis of all the data presented above, there are two possibilities:

(1) The mechanism for the intramolecular hydroamination of **3a–c** with **1-(CH<sub>2</sub>Ph)<sub>2</sub>** is analogous to that proposed by Marks et al. for the intramolecular hydroamination/cyclization of aminoalkenes mediated by lanthanide and actinide complexes.<sup>40</sup>

(2) The imido mechanism operates for the reactions of **1-(CH<sub>2</sub>Ph)<sub>2</sub>** and **1<sub>2</sub>-(μ-NPh)<sub>2</sub>** with **3a** and **3c**, and a change in mechanism occurs with **3b**.

On the basis of our experimental data, it is not possible to distinguish between the two situations.

## Conclusions

The uranium complex **1-(CH<sub>2</sub>Ph)<sub>2</sub>** acts as a precatalyst for both inter- and intramolecular hydroamination reactions. The interpretation of results from both kinetics and reactivity studies is consistent with more than one mechanism in the two types of reactions: uranium can behave similarly to group 4 metal complexes and access an imido mechanism or to lanthanides and access an amido mechanism. It is possible that (1) for the intermolecular hydroamination, the reaction between **1-(CH<sub>2</sub>Ph)<sub>2</sub>** and aniline forms the bridging-imide diuranium(IV) complex **1<sub>2</sub>-(μ-NPh)<sub>2</sub>** in a fast pre-equilibrium, the rate-determining step is the formation of the terminal imide, and a fast [2+2] cycloaddition reaction between the imide and the alkyne follows; (2) for the intramolecular hydroamination/cyclization, the reaction between **1-(CH<sub>2</sub>Ph)<sub>2</sub>** and the aminoalkene forms a bis(amide) fast, it is followed by a slow migratory-insertion step, and it concludes with a fast protonolysis reaction to give the cyclized product. Specific behaviors, such as the reaction between **1-(CH<sub>2</sub>Ph)<sub>2</sub>** and a secondary aminoalkene in an intramolecular hydroamination/cyclization, or the lack of reactivity of **1-(CH<sub>2</sub>Ph)<sub>2</sub>** with secondary amines and a terminal alkyne in an intermolecular hydroamination, signal that a change in mechanism could take place between the two types of reactions. A change in the mechanism, however, may occur as a response to steric factors. In favor of the first scenario (change in mechanism from the inter- to the intramolecular hydroamination) is the fact that the bridging-imide diuranium(IV) precursor (**1<sub>2</sub>-(μ-NPh)<sub>2</sub>**) behaved similarly to **1-(CH<sub>2</sub>Ph)<sub>2</sub>** toward aniline or secondary amines and Me<sub>3</sub>Si–C≡CH, while the benzyl-aryloxide complex **1-(CH<sub>2</sub>Ph)(OAr)** did not react with aniline and Me<sub>3</sub>Si–C≡CH. On the other hand, **1-(CH<sub>2</sub>Ph)(OAr)** did allow the complete conversion to the respective products of the intramolecular hydroamination/cyclization substrates **3a** and **3c**, indicating that the formation of a uranium-imide intermediate was not required for those reactions. Unfortunately, kinetics data, deuterium-labeling studies, and reactivity results were not sufficient to distinguish between all the reasonable pathways. The results of several experiments carried out to support the proposal that the mechanism changes based on the type of reaction (inter- versus intramolecular) were weakened by an abrupt change in the reactivity of the respective uranium

precursors and by the fact that the kinetics data are consistent with either possibility operating for both types of reactions. DFT calculations may be able to distinguish between these possibilities, although the paramagnetic nature of the catalytic species involved will complicate the interpretation of the results. It is interesting to point out that the ability to access multiple reaction mechanisms makes uranium an especially versatile catalyst for hydroamination reactions.

### Experimental Section

All experiments were performed under a dry nitrogen atmosphere using standard Schlenk techniques or an MBraun inert-gas glovebox. Solvents were purified using a two-column solid-state purification system by the method of Grubbs<sup>87</sup> and transferred to the glovebox without exposure to air. NMR solvents were obtained from Cambridge Isotope Laboratories, degassed, and stored over activated molecular sieves prior to use. Compounds **1-(CH<sub>2</sub>Ph)<sub>2</sub>**,<sup>56</sup> 2,2-diphenyl-4-penten-1-amine (**3a**),<sup>88</sup> *N*-methyl-2,2-diphenyl-4-penten-1-amine (**3b**),<sup>39</sup> 2,2-diphenyl-4-pentyn-1-amine (**3c**),<sup>88</sup> C<sub>6</sub>H<sub>5</sub>ND<sub>2</sub>,<sup>89</sup> and *3a-d*<sup>89</sup> were synthesized according to published procedures. Aniline, *N*-methylaniline, <sup>n</sup>Bu<sub>2</sub>NH, Me<sub>3</sub>Si-C≡CH, styrene, methylphenylacetylene, phenylacetylene, 2-butyne, *n*-butylamine, 1-hexyne, *tert*-butylacetylene, diphenylacetylene, 2,6-di-isopropylphenol, 2,6-dimethylphenol, and dimethylphenylphosphine were distilled under argon over CaH<sub>2</sub> and stored over sieves in the glovebox prior to use. Norbornylene was sublimed under argon and stored in the glovebox. 2,6-Di-*tert*-butylphenol was recrystallized from concentrated hexanes at -36 °C. <sup>1</sup>H NMR spectra were recorded on Bruker300 or Bruker500 spectrometers at room temperature in C<sub>6</sub>D<sub>6</sub> (the UCLA NMR spectrometers are supported by the NSF grant CHE-9974928). Chemical shifts are reported with respect to internal solvent, 7.16 ppm (C<sub>6</sub>D<sub>6</sub>). UV-vis-NIR spectra were recorded on a Varian Carey 5000 spectrophotometer from 200 to 1800 nm using matched, 1 cm quartz cells; all spectra were obtained using a solvent reference blank in a cuvette fitted with an air-free Teflon adapter. High-resolution mass spectrometry, ESI, was performed by the UCLA MIC Mass Spectrometry Laboratory on an IonSpec Ultima 7T FT-ICR-MS. CHN analyses were performed by UC Berkeley Micro-Mass facility, 8 Lewis Hall, College of Chemistry, University of California, Berkeley, CA 94720.

**Synthesis of I<sub>2</sub>-(μ-NPh)<sub>2</sub>**. Aniline (0.0077 g, 0.0827 mmol) was added to **1-(CH<sub>2</sub>Ph)<sub>2</sub>** (0.068 g, 0.079 mmol) in hexanes, at room temperature, and the reaction was stirred for 2 h. The volatiles were removed under reduced pressure, and hexanes was added to the resulting solid. The volatiles were removed again under reduced pressure, and recrystallization from a concentrated *n*-pentane solution at -36 °C afforded the product. Yield: 0.035 g, 56%. There are no observable peaks at room temperature in the <sup>1</sup>H NMR spectrum. <sup>1</sup>H NMR (500 MHz, 100 °C, toluene-*d*<sub>8</sub>), δ (ppm): 8.12 (s, 8H, C<sub>5</sub>H<sub>4</sub>), 4.87 (s, 36H, CCH<sub>3</sub>), -2.73 (s, 24H, SiCH<sub>3</sub>), -3.46 (s, 4H, NC<sub>6</sub>H<sub>5</sub>), -4.93 (s, 2H, NC<sub>6</sub>H<sub>5</sub>), -13.18 (s, 4H, C<sub>5</sub>H<sub>4</sub>), -35.88 (s, 4H, C<sub>5</sub>H<sub>4</sub>); the *o*-NC<sub>6</sub>H<sub>5</sub> peaks were not observed in the spectrum. Anal. Calcd (%) for C<sub>56</sub>H<sub>86</sub>Fe<sub>2</sub>-N<sub>6</sub>Si<sub>4</sub>U<sub>2</sub>·0.5(C<sub>5</sub>H<sub>12</sub>): C, 44.48; H, 5.87; N, 5.32. Found: C, 44.36; H, 5.64; N, 5.40.

**Synthesis of 1-(CH<sub>2</sub>Ph)(OAr)**. 2,6-Di-*tert*-butylphenol (0.048 g, 0.23 mmol) was added to **1-(CH<sub>2</sub>Ph)<sub>2</sub>** (0.068 g, 0.079 mmol) in toluene at room temperature, and the reaction was stirred for 4 h at 70 °C. The volatiles were removed under reduced pressure, the product was extracted with hexanes, and the volatiles were

removed again to give an analytically pure solid. Yield: 0.220 g, 97%. <sup>1</sup>H NMR (300 MHz, 25 °C, C<sub>6</sub>D<sub>6</sub>), δ (ppm): 54.62 (s, 6H, SiCH<sub>3</sub>), 45.75 (s, 6H, SiCH<sub>3</sub>), 35.17 (s, 18H, CCH<sub>3</sub>), -2.17 (t, 1H, OC<sub>6</sub>H<sub>3</sub> or C<sub>6</sub>H<sub>5</sub>), -5.60 (s, 2H, OC<sub>6</sub>H<sub>3</sub> or C<sub>6</sub>H<sub>5</sub>), -6.68 (s, 1H, OC<sub>6</sub>H<sub>3</sub> or C<sub>6</sub>H<sub>5</sub>), -7.47 (t, 1H, OC<sub>6</sub>H<sub>3</sub> or C<sub>6</sub>H<sub>5</sub>), -8.65 (s, 1H, OC<sub>6</sub>H<sub>3</sub> or C<sub>6</sub>H<sub>5</sub>), -17.20 (s, 2H, OC<sub>6</sub>H<sub>3</sub> or C<sub>6</sub>H<sub>5</sub>), -18.66 (d, 4H, C<sub>5</sub>H<sub>4</sub>), -31.31 (s, 9H, CCH<sub>3</sub>), -36.37 (s, 2H, C<sub>5</sub>H<sub>4</sub>), -38.95 (s, 2H, C<sub>5</sub>H<sub>4</sub>), -42.73 (s, 9H, CCH<sub>3</sub>); Ph-CH<sub>2</sub> was not observed in the spectrum. Anal. Calcd for C<sub>43</sub>H<sub>66</sub>Fe-N<sub>2</sub>OSi<sub>2</sub>U: C, 52.86; H, 6.81; N, 2.87. Found: C, 52.63; H, 6.97; N, 2.62.

**Synthesis of 1-(NHPH)(OAr)**. Aniline (0.021 g, 0.23 mmol) was added to **1-(CH<sub>2</sub>Ph)(OAr)** (0.233 g, 0.23 mmol) in toluene at room temperature, and the reaction mixture was stirred for 4 h at 70 °C. The volatiles were removed under reduced pressure, the product was extracted with hexanes, and the volatiles were removed again. The resulting solid was recrystallized from concentrated hexanes at -36 °C. Yield: 0.162 g, 72.9%. <sup>1</sup>H NMR (300 MHz, 25 °C, C<sub>6</sub>D<sub>6</sub>), δ (ppm): 36.57 (s, 6H, SiCH<sub>3</sub>), 32.06 (s, 6H, SiCH<sub>3</sub>), 24.61 (s, 18H, CCH<sub>3</sub>), 2.42 (t, 1H, OC<sub>6</sub>H<sub>3</sub> or NC<sub>6</sub>H<sub>5</sub>), -0.56 (d, 2H, OC<sub>6</sub>H<sub>3</sub> or NC<sub>6</sub>H<sub>5</sub>), -1.92 (t, 1H, OC<sub>6</sub>H<sub>3</sub> or NC<sub>6</sub>H<sub>5</sub>), -2.99 (s, 2H, OC<sub>6</sub>H<sub>3</sub> or NC<sub>6</sub>H<sub>5</sub>), -9.82 (s, 2H, OC<sub>6</sub>H<sub>3</sub> or NC<sub>6</sub>H<sub>5</sub>), -13.89 (s, 2H, OC<sub>6</sub>H<sub>3</sub> or NC<sub>6</sub>H<sub>5</sub>), -14.62 (s, 2H, OC<sub>6</sub>H<sub>3</sub> or NC<sub>6</sub>H<sub>5</sub>), -25.73 (s, 18H, CCH<sub>3</sub>), -27.86 (s, 2H, OC<sub>6</sub>H<sub>3</sub> or NC<sub>6</sub>H<sub>5</sub>), -37.03 (s, 2H, OC<sub>6</sub>H<sub>3</sub> or NC<sub>6</sub>H<sub>5</sub>). Anal. Calcd for C<sub>42</sub>H<sub>65</sub>FeN<sub>3</sub>OSi<sub>2</sub>U·0.33(C<sub>6</sub>H<sub>14</sub>): C, 52.49; H, 6.97; N, 4.17. Found: C, 52.41; H, 7.00; N, 3.79.

**Synthesis of 2,2-Diphenyl-4-pentyn-1-amine (3c)**. Diphenylacetonitrile (4.0 g, 20.7 mmol) in DMF was added to a stirring DMF slurry of NaH (0.521 g, 21.7 mmol) at room temperature, under argon. After 1 h, the solution was cooled to 0 °C, and propargyl bromide (1.78 mL, 20.7 mmol) was added. The reaction was allowed to warm to room temperature and stirred overnight. The product was extracted with benzene, washed with water, and dried over MgSO<sub>4</sub>. The volatiles were then removed under reduced pressure, yielding a slightly yellow oil (4.2 g, 18.2 mmol, 89% yield). The product was added to a stirring diethyl ether slurry of LiAlH<sub>4</sub> (1.05 g, 27.6 mol) under argon, at 0 °C. After stirring at room temperature overnight, the reaction mixture was cooled to -78 °C and quenched with 6 M NaOH. The product was extracted with diethyl ether (2.9 g, 12.3 mmol) and purified by column chromatography using a 3:1 ethyl acetate/hexanes mixture by volume. The product was dried overnight, resulting in a white powder, which was recrystallized from diethyl ether/hexanes at -36 °C (1.0 g, 4.5 mmol, 24% yield). <sup>1</sup>H NMR (500 MHz, 25 °C, CDCl<sub>3</sub>), δ (ppm): 7.3-7.2 (m, 10H, C<sub>6</sub>H<sub>5</sub>), 3.54 (s, 2H, NH<sub>2</sub>CH<sub>2</sub>), 3.11 (d, 2H, CHCH<sub>2</sub>), 1.94 (t, 1H, CHCH<sub>2</sub>), 0.99 (s, 2H, CH<sub>2</sub>NH<sub>2</sub>). <sup>13</sup>C NMR (75 MHz, 25 °C, CDCl<sub>3</sub>), δ (ppm): 145.24 (Ph-C), 128.08 (*meta*-Ph-CH), 128.01 (*ortho*-Ph-CH), 126.38 (*para*-Ph-CH), 81.42 (HCCCH<sub>2</sub>), 71.48 (HCCCH<sub>2</sub>), 51.28 (NH<sub>2</sub>CH<sub>2</sub>), 49.13 (NH<sub>2</sub>CH<sub>2</sub>C), 27.74 (HCCCH<sub>2</sub>). HRMS, ESI: calcd 236.1439, found 236.1434.

**X-ray Crystal Structures.** The X-ray data collections were carried out on a Bruker AXS single-crystal X-ray diffractometer using Mo Kα radiation and a SMART APEX CCD detector. The data were reduced by SAINTPLUS, and an empirical absorption correction was applied using the package SADABS. The structures were solved and refined using SHELXTL (Bruker 1998, SMART, SAINT, XPREP, AND SHELXTL, Bruker AXS Inc., Madison, WI).<sup>90</sup> All atoms were refined anisotropically, and hydrogen atoms were placed in calculated positions unless specified otherwise. Tables with atomic coordinates and equivalent isotropic displacement parameters, with all the bond lengths and angles, and with anisotropic displacement parameters are listed in the Supporting Information.

**X-ray Crystal Structure of I<sub>2</sub>-(μ-NPh)<sub>2</sub>**. X-ray quality crystals were obtained from a concentrated *n*-pentane solution placed in

(87) Pangborn, A. B.; Giardello, M. A.; Grubbs, R. H.; Rosen, R. K.; Timmers, F. J. *Organometallics* **1996**, *15*, 1518.

(88) Bender, C. F.; Widenhoefer, R. A. *J. Am. Chem. Soc.* **2005**, *127*, 1070.

(89) Gagne, M. R.; Stern, C. L.; Marks, T. J. *J. Am. Chem. Soc.* **1992**, *114*, 275.

(90) Sheldrick, G. *Acta Crystallogr. A* **2008**, *64*, 112.

a  $-35\text{ }^{\circ}\text{C}$  freezer in the glovebox. Inside the glovebox, the crystals were coated with oil (STP Oil Treatment) on a microscope slide, which was brought outside the glovebox. A total of 62 937 reflections ( $-35 \leq h \leq 35$ ,  $-26 \leq k \leq 25$ ,  $-18 \leq l \leq 18$ ) were collected at  $T = 100(2)\text{ K}$  with  $2\theta_{\text{max}} = 61.66^{\circ}$ , of which 18 594 were unique ( $R_{\text{int}} = 0.0321$ ). The unit cell contained solvent molecules that were too disordered to model. As a consequence, the PLATON SQUEEZE program was used to remove the solvent from the unit cell. The residual peak and hole electron density were  $1.60$  and  $-1.01\text{ e } \text{\AA}^{-3}$ , respectively. The least-squares refinement converged normally with residuals of  $R_1 = 0.0295$  and  $\text{GOF} = 1.048$ . Crystal and refinement data for **1**<sub>2</sub>-( $\mu$ -NPh)<sub>2</sub>: formula  $\text{C}_{56}\text{H}_{85}\text{N}_6\text{Fe}_2\text{Si}_4\text{U}_2$ , space group  $P2(1)/c$ ,  $a = 25.323(3)\text{ \AA}$ ,  $b = 18.607(2)\text{ \AA}$ ,  $c = 13.5646(14)\text{ \AA}$ ,  $\beta = 97.009(1)^{\circ}$ ,  $V = 6343.6(11)\text{ \AA}^3$ ,  $Z = 4$ ,  $\mu = 5.652\text{ mm}^{-1}$ ,  $F(000) = 3020$ ,  $R_1 = 0.0443$  and  $wR_2 = 0.0703$  (based on all 18 594 data).

**X-ray Crystal Structure of 1-(CH<sub>2</sub>Ph)(OAr).** X-ray quality crystals were obtained from a concentrated Et<sub>2</sub>O solution placed in a  $-35\text{ }^{\circ}\text{C}$  freezer in the glovebox. Inside the glovebox, the crystals were coated with oil (STP Oil Treatment) on a microscope slide, which was brought outside the glovebox. A total of 40 674 reflections ( $-16 \leq h \leq 16$ ,  $-31 \leq k \leq 31$ ,  $-21 \leq l \leq 20$ ) were collected at  $T = 100(2)\text{ K}$  with  $2\theta_{\text{max}} = 58.13^{\circ}$ , of which 11 371 were unique ( $R_{\text{int}} = 0.0390$ ). The residual peak and hole electron density were  $0.85$  and  $-0.61\text{ e } \text{\AA}^{-3}$ , respectively. The least-squares refinement converged normally with residuals of  $R_1 = 0.0268$  and  $\text{GOF} = 1.011$ . Crystal and refinement data for **1**-(CH<sub>2</sub>Ph)(OAr): formula  $\text{C}_{43}\text{H}_{66}\text{N}_2\text{FeSi}_2\text{OU}$ , space group  $P2(1)/n$ ,  $a = 12.1124(13)\text{ \AA}$ ,  $b = 23.245(3)\text{ \AA}$ ,  $c = 15.3884(17)\text{ \AA}$ ,  $\beta = 98.859(1)^{\circ}$ ,  $V = 4280.9(8)\text{ \AA}^3$ ,  $Z = 4$ ,  $\mu = 4.206\text{ mm}^{-1}$ ,  $F(000) = 1968$ ,  $R_1 = 0.0391$  and  $wR_2 = 0.0579$  (based on all 11 371 data).

**Magnetic-Susceptibility Measurements.** Measurements for **1**<sub>2</sub>-( $\mu$ -NPh)<sub>2</sub> were carried out on batches obtained independently until at least two different experiments gave superimposable results. Magnetic susceptibility measurements were recorded using a SQUID magnetometer at  $5000\text{ G}$ . The samples were prepared in the glovebox (ca.  $50\text{ mg}$ ), loaded in a gelatin capsule that was positioned inside a plastic straw, and carried to the magnetometer in a tube under N<sub>2</sub>. The sample was quickly inserted into the instrument and centered, and data were obtained from  $5$  to  $300\text{ K}$ . The contribution from the sample holders was not accounted for. Effective magnetic moments were calculated by using the formula  $2.828(T\chi_{\text{mol}})^{1/2}$  for non-Curie–Weiss behavior.

**Diffusion-Coefficient Experiment.** The pulse-gradient, spin-echo (SE:  $90^{\circ}-t_1-180^{\circ}-t_1$ -echo) technique was used to measure the self-diffusion coefficient of **1**<sub>2</sub>-( $\mu$ -NPh)<sub>2</sub> in toluene-*d*<sub>8</sub> at  $100\text{ }^{\circ}\text{C}$  on a Bruker DRX-500 NMR spectrometer. The gradient strength was measured running the pulse-gradient spin-echo experiment on H<sub>2</sub>O and using the literature value of  $2.3 \times 10^{-9}\text{ m}^2/\text{s}$  for the self-diffusion coefficient. The gradient strength was found to be  $51.0\text{ G/cm}$ . The time during which the diffusion process occurred was varied from  $50\text{ }\mu\text{s}$  to  $5\text{ ms}$ . The duration of the gradient pulse ( $\delta$ ) was set to  $1\text{ ms}$ . The hydrodynamic radius was obtained by using the Stokes–Einstein equation.<sup>68</sup>

**Hydroamination Reactions.** In the glovebox, **1**-(CH<sub>2</sub>Ph)<sub>2</sub>, the alkyne, the amine, and the internal standard, hexaethylbenzene, were added to C<sub>6</sub>D<sub>6</sub> and transferred to a Teflon-sealed NMR tube, which was taken out of the glovebox. The tube was placed

in a  $70\text{ }^{\circ}\text{C}$  oil bath, and the reactions were monitored by <sup>1</sup>H NMR spectroscopy. The <sup>1</sup>H NMR spectra of the products were compared with those reported in the literature.<sup>33,36,52,91</sup>

**Kinetics Studies.** In the glovebox, **1**-(CH<sub>2</sub>Ph)<sub>2</sub>, the alkyne, the amine, and the internal standard, hexaethylbenzene, were added to a Teflon-sealed NMR tube in C<sub>6</sub>D<sub>6</sub>. The NMR tube was inserted into the instrument (Bruker AV300) and heated to  $70\text{ }^{\circ}\text{C}$ . The reactions were monitored until ca. 90% conversion. For the intermolecular reaction, the aniline concentration was  $0.16\text{ M}$ , and for the intramolecular reaction the **3a** concentration was  $0.42\text{ M}$ . Errors for the activation parameters were calculated as reported in the literature.<sup>92,93</sup>

**Large-Scale Reaction of Aniline and Me<sub>3</sub>Si–C≡CH with 1-(CH<sub>2</sub>Ph)<sub>2</sub>.** **1**-(CH<sub>2</sub>Ph)<sub>2</sub> ( $0.023\text{ g}$ ,  $0.027\text{ mmol}$ ) in  $4\text{ mL}$  of toluene was added to aniline ( $0.200\text{ g}$ ,  $2.14\text{ mmol}$ ) and Me<sub>3</sub>Si–C≡CH ( $0.263\text{ g}$ ,  $2.67\text{ mmol}$ ) in  $8\text{ mL}$  of toluene in a Schlenk tube. The reaction was heated at  $70\text{ }^{\circ}\text{C}$  and monitored by <sup>1</sup>H NMR spectroscopy by analyzing aliquots from the reaction. When the conversion to product was at least 90%, the volatiles were removed under reduced pressure and the product **2** was isolated by Kugelrohr distillation. Yield:  $0.306\text{ g}$ ,  $74.4\%$ .

**Large-Scale Reaction of 3a with 1-(CH<sub>2</sub>Ph)<sub>2</sub>.** **1**-(CH<sub>2</sub>Ph)<sub>2</sub> ( $0.024\text{ g}$ ,  $0.028\text{ mmol}$ ) in  $1\text{ mL}$  of toluene was added to **3a** ( $0.350\text{ g}$ ,  $1.56\text{ mmol}$ ) in  $2.5\text{ mL}$  of toluene in a Schlenk tube. The reaction was heated at  $70\text{ }^{\circ}\text{C}$  and monitored by <sup>1</sup>H NMR spectroscopy by analyzing aliquots from the reaction. When the conversion to product was at least 90%, the volatiles were removed under reduced pressure and the product **4a** was isolated by Kugelrohr distillation. Yield:  $0.276\text{ g}$ ,  $79.0\%$ .

**Kinetic-Isotope Effect for the Intermolecular-Hydroamination Reaction.** In the glovebox, **1**-(CH<sub>2</sub>Ph)<sub>2</sub> ( $0.85\text{ mg}$ ,  $9.8 \times 10^{-4}\text{ mmol}$ ), aniline ( $6.5\text{ mg}$ ,  $0.069\text{ mmol}$ ), Me<sub>3</sub>Si–C≡CH ( $110\text{ mg}$ ,  $1.12\text{ mmol}$ ), and hexaethylbenzene ( $0.75\text{ mg}$ ,  $3.04 \times 10^{-3}\text{ mmol}$ ) in a total volume of  $0.4\text{ mL}$  of C<sub>6</sub>D<sub>6</sub> were added to a J.-Young tube. Another J.-Young tube was set up identically and simultaneously to the previous reaction using C<sub>6</sub>H<sub>5</sub>ND<sub>2</sub>. The reactions were monitored by <sup>1</sup>H NMR spectroscopy.

**Kinetic-Isotope Effect for the Intramolecular-Hydroamination Reaction.** In the glovebox, **1**-(CH<sub>2</sub>Ph)<sub>2</sub> ( $2.6\text{ mg}$ ,  $3 \times 10^{-3}\text{ mmol}$ ), **3a** ( $40\text{ mg}$ ,  $0.069\text{ mmol}$ ), and hexaethylbenzene ( $3.0\text{ mg}$ ,  $0.012\text{ mmol}$ ) in a total volume of  $0.4\text{ mL}$  of C<sub>6</sub>D<sub>6</sub> were added to a J. Young tube. Another J. Young tube was set up identically and simultaneously to the previous reaction using **3a-d**<sub>2</sub>. The reactions were monitored by <sup>1</sup>H NMR spectroscopy.

**Acknowledgment.** The authors thank Marisa J. Monreal for help with the SQUID experiments, Gregory Kuzmanich for help with the absorption-spectroscopy experiments, Dr. Robert Taylor for assistance with the diffusion-coefficient experiment, and Prof. Kai Hultsch (Rutgers University) for insightful discussions. This work was supported by the UCLA, Sloan Foundation, and DOE (Grant ER15984).

**Supporting Information Available:** Details of the NMR spectroscopy experiments, DFT calculations, and full crystallographic descriptions (in cif format) are available free of charge via the Internet at <http://pubs.acs.org>.

(91) Gribkov, D. V.; Hultsch, K. C.; Hampel, F. *J. Am. Chem. Soc.* **2006**, *128*, 3748.

(92) Morse, P. M.; Spencer, M. D.; Wilson, S. R.; Girolami, G. S. *Organometallics* **2002**, *13*, 1646.

(93) Steigel, A.; Sauer, J.; Kleier, D. A.; Binsch, G. *J. Am. Chem. Soc.* **2002**, *94*, 2770.